

RESEARCH ARTICLE

Spatial Patterns of a Predator-Prey System of Leslie Type with Time Delay

Caiyun Wang^{1*}, Lili Chang², Huifeng Liu³

1 Department of Mathematics, Xinzhou Teachers University, Xinzhou 034000, Shan'xi, China, **2** Complex Systems Research Center, Shanxi University, Taiyuan, Shanxi 030006, China, **3** College of Material Science and Engineering, Taiyuan University of Science and Technology, Taiyuan 030024, Shan'xi, China

* xzwcyl234@163.com



Abstract

Time delay due to maturation time, capturing time or other reasons widely exists in biological systems. In this paper, a predator-prey system of Leslie type with diffusion and time delay is studied based on mathematical analysis and numerical simulations. Conditions for both delay induced and diffusion induced Turing instability are obtained by using bifurcation theory. Furthermore, a series of numerical simulations are performed to illustrate the spatial patterns, which reveal the information of density changes of both prey and predator populations. The obtained results show that the interaction between diffusion and time delay may give rise to rich dynamics in ecosystems.

OPEN ACCESS

Citation: Wang C, Chang L, Liu H (2016) Spatial Patterns of a Predator-Prey System of Leslie Type with Time Delay. PLoS ONE 11(3): e0150503. doi:10.1371/journal.pone.0150503

Editor: Gui-Quan Sun, Shanxi University, CHINA

Received: January 4, 2016

Accepted: February 16, 2016

Published: March 1, 2016

Copyright: © 2016 Wang et al. This is an open access article distributed under the terms of the [Creative Commons Attribution License](https://creativecommons.org/licenses/by/4.0/), which permits unrestricted use, distribution, and reproduction in any medium, provided the original author and source are credited.

Data Availability Statement: All relevant data are within the paper and its Supporting Information files.

Funding: This research is supported by the Youth Foundation of Shan'Xi Province under Grant 2015021020 and the Key Construction Disciplines Project of Xinzhou Normal University XK201501. The funders had no role in study design, data collection and analysis, decision to publish, or preparation of the manuscript.

Competing Interests: The authors have declared that no competing interests exist.

Introduction

Thanks to the classical work of Lotka (in 1925) and Volterra (in 1926), modeling predator-prey interaction system has become one of the hot issues in mathematical ecology [1–6]. As is well known, one of the principles that predator-prey models follow is that predators can grow as a function of what they have eaten [7]. One of the famous functional response function is Generalized Holling type III [8]. When $b = 0$, it is called Holling type III. Moreover, not only is the predator growth term described by a function of the prey density, but also is described as a function of the ratio of predator and their prey, y/x , where x and y stand for prey and predator density respectively, see for example [9, 10]. The predator-prey system takes the following form:

$$\begin{cases} \frac{dx}{d\tau} = xg(x, K) - yp(x), \\ \frac{dy}{d\tau} = yq\left(\frac{y}{x}\right), \end{cases} \quad (1)$$

where $g(x, K)$ describes the specific rate of the prey if there is no predator. $p(x)$ is the functional response function which describes the change in the density of the prey when they are attacked by per predator in per unit time. Information about the properties of function $g(x, K)$, $p(x)$ and $q(x)$ are available in [11, 12]. In this paper, we consider [system \(1\)](#) with the following functions,

$g(x, K) = r(x - \frac{x}{K}), p(x) = \frac{mx^2y}{ax^2+1}$ and $q(x) = y\theta(1 - \frac{hy}{x})$, namely, the predator-prey system of Leslie type with Holling type III functional response. Then Eq (1) becomes:

$$\begin{cases} \frac{dx}{d\tau} = rx\left(1 - \frac{x}{K}\right) - \frac{mx^2y}{ax^2+1}, \\ \frac{dy}{d\tau} = y\theta\left(1 - \frac{hy}{x}\right), \end{cases} \tag{2}$$

where the parameter r, K, a, θ, m and h are all positive constants. r is the prey intrinsic growth rate. K is the carrying capacity. m is capturing rate. a is half capturing rate. θ is predator intrinsic growth rate. h is conversion rate of prey into predator biomass. For the sake of convenience, system (2) should be rewritten into the nondimensional form. Assuming

$$u = \frac{x}{K}, \quad v = \frac{mky}{r}, \quad t = r\tau, \quad \eta = \frac{\theta}{r}, \quad \epsilon = ak^2, \quad \gamma = \frac{hr}{mk^2},$$

then system (2) becomes:

$$\begin{cases} \frac{du}{dt} = u(1 - u) - \frac{u^2v}{\epsilon u^2 + 1} := f(u, v), \\ \frac{dv}{dt} = v\eta\left(1 - \frac{\gamma v}{u}\right) := g(u, v) := v\eta[1 - q(u, v)]. \end{cases} \tag{3}$$

Pattern formation in reaction-diffusion system is one of the attractive problems in natural, social, and technological sciences. Espatially in ecological system, various predator-prey models with diffusion have been studied [13–18]. Pattern formation can well explain species survival under the influence of individual mobility. Combing Eq (3) with diffusion, we have the spatio-temporal predator-prey system of Leslie type with Holling type III functional response:

$$\begin{cases} \frac{\partial u}{\partial t} = u(1 - u) - \frac{u^2v}{\epsilon u^2 + 1} + D_1 \nabla^2 u, \\ \frac{\partial v}{\partial t} = v\eta\left(1 - \frac{\gamma v}{u}\right) + D_2 \nabla^2 v, \end{cases} \tag{4}$$

where the positive constants D_1 and D_2 denote the diffusive coefficients of u and v , respectively. $\nabla^2 = \frac{\partial^2}{\partial x^2} + \frac{\partial^2}{\partial y^2}$ is the usual Laplacian operator in two-dimensional space, which describes the random motion.

On the other hand, time delay due to maturation time, capturing time, gestation or other reasons widely exists and plays an important role in many biological dynamical systems [19, 20]. In order to reflect the current population dynamics, the rate of change of which depends on the past population of the system, we should incorporate time delays into mathematical models [21–24]. Although a lot of work has been done about the spatial predator-prey model [25–28] and studies of delay feedback on pattern formation have achieved great progress [29–33], study of delay driven pattern formation in a Leslie type system with Holling type III functional response seems to be rare. As a result, in the present paper we aim to study the effects of time delay on the spatiotemporal dynamics of a Leslie type model with Holling type III

functional response. The model is as following form:

$$\begin{cases} \frac{\partial u}{\partial t} = u(1 - u) - \frac{u^2 v}{\epsilon u^2 + 1} + D_1 \nabla^2 u, \\ \frac{\partial v}{\partial t} = v\eta \left[1 - \frac{\gamma v(t - \tau)}{u(t - \tau)} \right] + D_2 \nabla^2 v, \end{cases} \quad (5)$$

where $\tau > 0$ is a constant due to the negative feedback. Let Ω be a square flat domain. The initial conditions are

$$u(x, y; t) > 0, \quad v(x, y; t) > 0, \quad (x, y) \in \Omega = (0, L) \times (0, L) \quad \text{with} \quad t \in [-\tau, 0]. \quad (6)$$

Generally speaking, to make sure that Turing pattern is determined by reaction-diffusion mechanism, we usually choose zero-flux boundary conditions

$$\frac{\partial u}{\partial n} \Big|_{(x,y)} = \frac{\partial v}{\partial n} \Big|_{(x,y)} = 0, \quad (7)$$

which means that there is no flux of populations through the boundary, i.e., no external input is imposed from outside.

This paper is organized as follows. In section 2, we study the dynamics of model without delay. In section 3, we obtain the condition of Turing instability (diffusion and delay induced instabilities) via linear stability analysis. In section 4, we present various spatial patterns by performing numerical simulations. Finally, we give some conclusions and discussions in section 5.

Materials and Methods

Existence of positive equilibria

We need to analyze the stability criteria of [model \(5\)](#) without delay and diffusion. The corresponding model is [system \(3\)](#). Obviously, [system \(3\)](#) has equilibrium $E_0 = (1, 0)$, which corresponds to extinction of the predator. From the biological point of view, we are interested in the interior equilibria points, which are the positive solutions of the following cubic polynomial equations of the [system \(3\)](#):

$$\begin{cases} (1 - u) - \frac{uv}{\epsilon u^2 + 1} = 0, \\ v = \frac{u}{\gamma}. \end{cases} \quad (8)$$

Substituting the second equality for the first equality in [Eq \(8\)](#), we have that:

$$F(u) := u^3 + \omega_2 u^2 + \omega_1 u + \omega_0 = 0, \quad (9)$$

where $\omega_2 = \frac{1}{\gamma\epsilon} - 1$, $\omega_1 = \frac{1}{\epsilon}$ and $\omega_0 = -\frac{1}{\epsilon} < 0$. The number of equilibria in [Eq \(3\)](#) is determined by the number of real roots of F in the interval $I_0 = (0, 1)$. In addition, $F'(u) = 3u^2 + 2\omega_2 u + \omega_1$ has two zeros

$$\xi_{\pm} = \frac{\gamma\epsilon - 1 \pm \sqrt{\Delta_1}}{3\epsilon\gamma}, \quad (10)$$

when

$$\Delta_1 := (\gamma\epsilon - 1)^2 - 3\epsilon\gamma^2 \geq 0. \quad (11)$$

The discriminant of the cubic polynomial F is given by

$$\Delta_2 := \left(\frac{Q}{2}\right)^2 + \left(\frac{P}{3}\right)^3, \tag{12}$$

where $P = \omega_1 - \omega_2^2/3$ and $Q = (2\omega_2^3 - 9\omega_1\omega_2 + 27\omega_0)/27$. Similar to Lemma 1 in [34], we have the following results.

[System \(3\)](#) has at least one equilibrium and at most three equilibria in the interval $I_0 = (0, 1)$. Moreover, consider the following condition:

$$0 < \xi_{\pm} < 1; \tag{13}$$

$$F(\xi_-) > 0 \text{ and } F(\xi_+) < 0; \tag{14}$$

$$\Delta_2 = 0; \tag{15}$$

$$0 < 2\sqrt[3]{\pm Q/2} - \gamma^2/3 < 1; \tag{16}$$

$$F(\xi_-)F(\xi_+) > 0; \tag{17}$$

$$\xi_{\pm} < 0. \tag{18}$$

1. If and only if Eqs (13) and (14) hold, then [system \(3\)](#) has three equilibria in the interval $I_0 = (0, 1)$.
2. If and only if Eqs (15) and (16) hold, [system \(3\)](#) two equilibria in the interval $I_0 = (0, 1)$.
3. If and only if Eqs (18), or(13) and (17) hold, [system \(3\)](#) has a unique equilibrium in the interval $I_0 = (0, 1)$ Moreover, if [system \(3\)](#) has a unique equilibrium $E_1(u_1^*, v_1^*)$ where $v_1^* = u_1^*/\gamma$, then u_1^* is either a simple zero of F or a zero of multiplicity 3 of F .

We describe qualitative properties and stability of the interior equilibria of [system \(3\)](#) (see [S1 File](#)). By the proof of **Theorem 1** (see [S1 File](#)), we have the following conclusion.

If

$$\text{tr}(J) = f_u + g_v < 0, \tag{19}$$

all of the positive equilibria of [system \(3\)](#) are stable, except the saddle (corresponds to the zero A of F in [Fig 1](#)) and degenerate equilibria (corresponds to the zeros B, C and D of F in [Figs 2](#) and [3](#) respectively).

Turing instability analysis of [model \(4\)](#)

In this subsection, we will give a brief analysis of Turing instability of [model \(4\)](#). For the sake of convenience, let $E^*(u^*, v^*)$ be anyone of the interior steady equilibrium in **Theorem 1** (see [S1 File](#)). The characteristic polynomial at $E^*(u^*, v^*)$ is

$$|\lambda E - J_k| = 0, \tag{20}$$

where $J_k = J - \text{diag}(D_1, D_2)k^2$, K is a wavenumber and J is the Jacobian matrix of [system \(3\)](#) at $E^*(u^*, v^*)$.

Further, [Eq \(20\)](#) yields

$$\lambda^2 - \text{tr}(J_k)\lambda + \det(J_k) = 0, \tag{21}$$

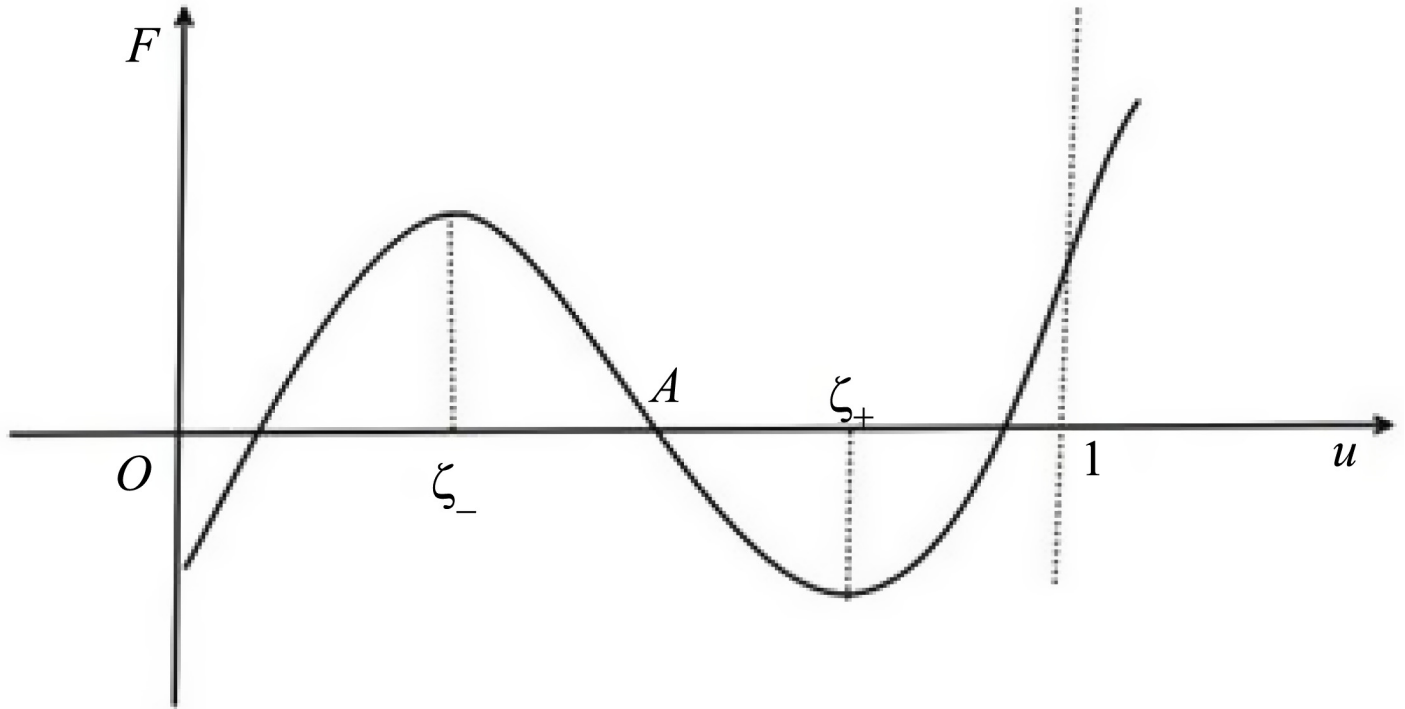


Fig 1. F has three zero solutions in I_0 .

doi:10.1371/journal.pone.0150503.g001

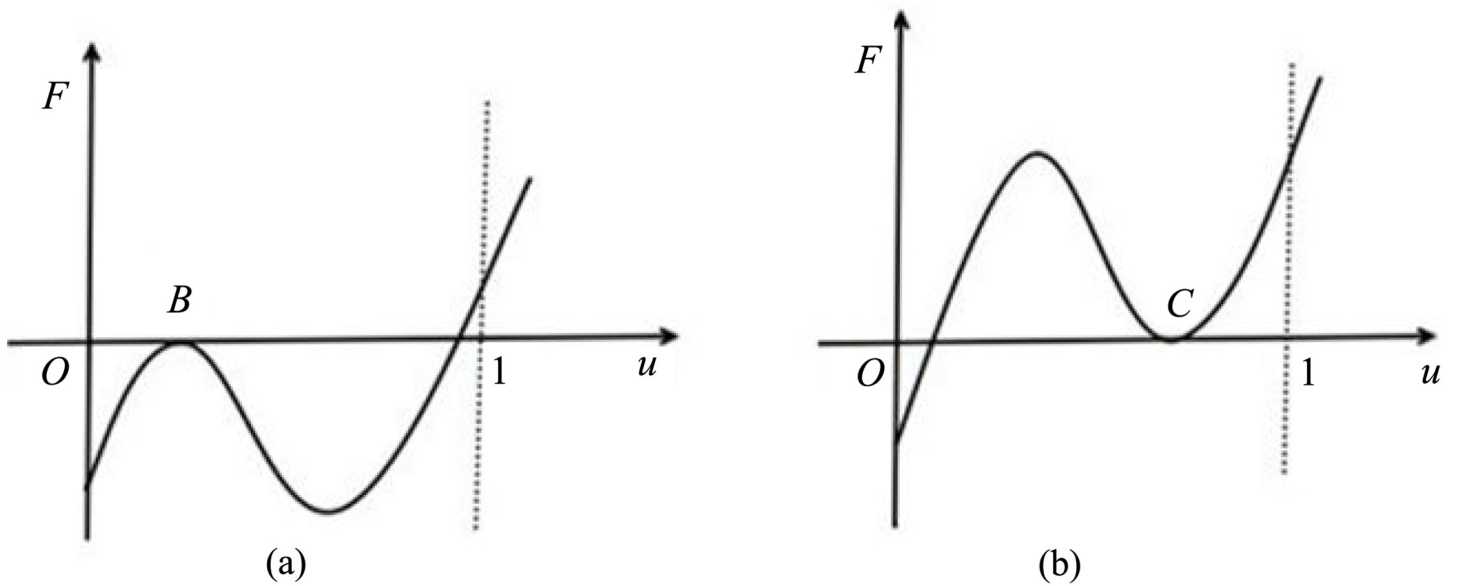


Fig 2. F has two zero solutions in I_0 .

doi:10.1371/journal.pone.0150503.g002

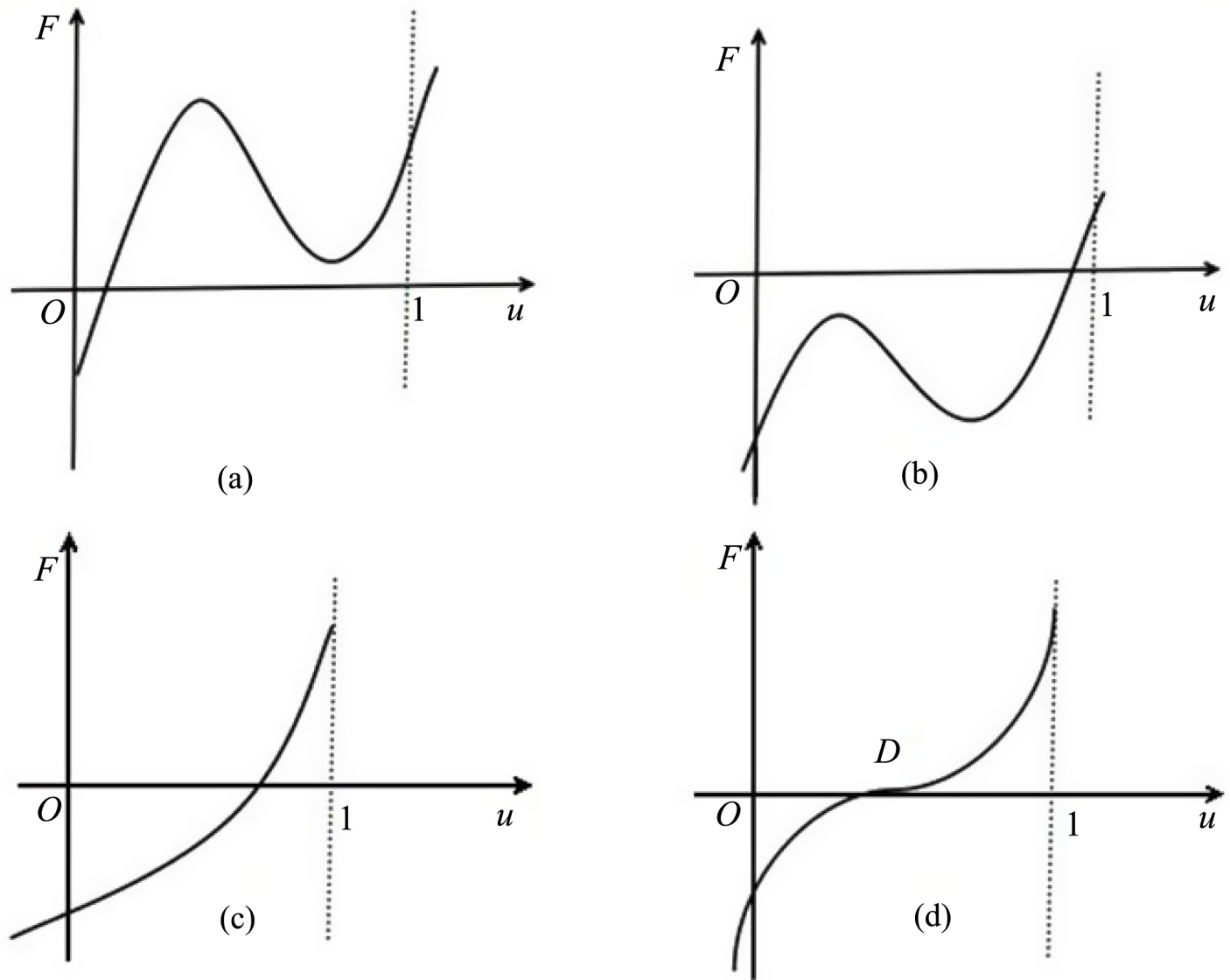


Fig 3. F has a unique zero solution in I_0 .

doi:10.1371/journal.pone.0150503.g003

where

$$\text{tr}(J_k) = \text{tr}(J) - (D_1 + D_2)k^2, \tag{22}$$

and

$$\det(J_k) = \det(J) + D_1D_2k^4 - (D_2f_u + D_1g_v)k^2. \tag{23}$$

We can get the roots of [Eq \(20\)](#):

$$\lambda_k = \frac{\text{tr}(J_k) \pm \sqrt{\text{tr}(J_k)^2 - 4\det(J_k)}}{2}. \tag{24}$$

The condition for the onset of Hopf instability holds when a pair of imaginary eigenvalues cross the real axis from the negative value to the positive one and there is no diffusion [35, 36]. That is to say, the Hopf bifurcation occurs when

$$\text{Im}(\lambda_k) \neq 0, \quad \text{Re}(\lambda_k) = 0 \quad \text{at } k = 0.$$

A homogeneously steady state is said to be Turing instability if it is stable for [model \(3\)](#) without diffusion but becomes unstable because of homogeneous perturbation caused by diffusion. A general linear analysis [37–39] show that the necessary conditions for onset of Turing instability for [model \(4\)](#) are given by condition [Eq \(19\)](#) and the following conditions

$$\det(J) = f_u g_v - f_v g_u > 0, \tag{25}$$

$$D_2 f_u + D_1 g_v > 0, \tag{26}$$

$$(D_2 f_u + D_1 g_v)^2 > 4D_1 D_2 (f_u g_v - f_v g_u). \tag{27}$$

The condition Eqs (19) and (25) make sure that the equilibrium $E^* = (u^*, v^*)$ is stable for [model \(3\)](#) without diffusion, and becomes unstable for [model \(4\)](#) if $\text{Re}(\lambda_k)$ transits the real axis from a negative side to a positive one (corresponding to condition [Eq \(26\)](#) and [\(27\)](#)). Namely, the Turing bifurcation occurs when

$$\text{Im}(\lambda_k) = 0, \quad \text{Re}(\lambda_k) = 0 \quad \text{at } k = k_T \neq 0,$$

and wavenumber k_T satisfies

$$k_T^2 = \sqrt{\frac{\det(J)}{D_1 D_2}}.$$

Results

Linear stability analysis

In this subsection, we will consider the stability of [model \(5\)](#). Obviously, [model \(5\)](#) has the same equilibria as [model \(4\)](#). Similar to [30, 31], assume that τ is small enough, then we replace $u(x, y, t - \tau) = u(x, y, t) - \tau \frac{\partial u(x, y, t)}{\partial t}$ and $v(x, y, t - \tau) = v(x, y, t) - \tau \frac{\partial v(x, y, t)}{\partial t}$ in [system \(5\)](#) and obtain the following equations:

$$\begin{cases} \frac{\partial u}{\partial t} = f(u, v) + D_1 \nabla^2 u, \\ \frac{\partial v}{\partial t} = v\eta \left[1 - q \left(u(x, y, t) - \tau \frac{\partial u(x, y, t)}{\partial t}, v(x, y, t) - \tau \frac{\partial v(x, y, t)}{\partial t} \right) \right] + D_2 \nabla^2 v. \end{cases} \tag{28}$$

Expanding [Eq \(28\)](#) in Taylor Series and neglecting the higher order non-linearities, then [Eq \(28\)](#) becomes:

$$\begin{cases} \frac{\partial u}{\partial t} = f(u, v) + D_1 \nabla^2 u, \\ \frac{\partial v}{\partial t} = v\eta \left[1 - q(u, v) + \tau q_u \frac{\partial u(x, y, t)}{\partial t} + \tau q_v \frac{\partial v(x, y, t)}{\partial t} \right] + D_2 \nabla^2 v, \end{cases} \tag{29}$$

where $q_u = \frac{\partial q}{\partial u}$ and $q_v = \frac{\partial q}{\partial v}$. By Eq (29), we obtain the following equations:

$$\begin{cases} \frac{\partial u}{\partial t} = f(u, v) + D_1 \nabla^2 u, \\ \frac{\partial v}{\partial t} = \frac{1}{1 - \nu \eta \tau q_v} g(u, v) + \frac{\nu \eta \tau q_u}{1 - \nu \eta \tau q_v} f(u, v) + \frac{\nu \eta \tau q_u}{1 - \nu \eta \tau q_v} D_1 \nabla^2 u + \frac{1}{1 - \nu \eta \tau q_v} D_2 \nabla^2 v. \end{cases} \quad (30)$$

If we take small spatiotemporal perturbations $\delta u(x, y, t)$ and $\delta v(x, y, t)$ on the steady state $E^* = (u^*, v^*)$ of system (5), then we have:

$$u(x, y, t) = u^* + \delta u(x, y, t), \quad v(x, y, t) = v^* + \delta v(x, y, t). \quad (31)$$

Expanding the reaction terms around the steady state $E^* = (u^*, v^*)$ in Taylor Series up to first order and rearranging the terms, we obtain:

$$\begin{cases} \frac{\partial(\delta u)}{\partial t} = f_u(\delta u) + f_v(\delta v) + D_1 \nabla^2(\delta u), \\ \frac{\partial(\delta v)}{\partial t} = \left(\frac{g_u}{1 - \nu^* \eta \tau q_v} + \frac{\nu^* \eta \tau q_u f_u}{1 - \nu^* \eta \tau q_v} \right) (\delta u) + \left(\frac{g_v}{1 - \nu^* \eta \tau q_v} + \frac{\nu^* \eta \tau q_u f_v}{1 - \nu^* \eta \tau q_v} \right) (\delta v) \\ \quad + \frac{\nu^* \eta \tau q_u D_1 \nabla^2(\delta u)}{1 - \nu^* \eta \tau q_v} + \frac{D_2 \nabla^2(\delta v)}{1 - \nu^* \eta \tau q_v}, \end{cases} \quad (32)$$

where $f_u = \frac{\partial f}{\partial u} |_{(u^*, v^*)}$, $f_v = \frac{\partial f}{\partial v} |_{(u^*, v^*)}$, $g_u = \frac{\partial g}{\partial u} |_{(u^*, v^*)}$, $g_v = \frac{\partial g}{\partial v} |_{(u^*, v^*)}$, $q_u = \frac{\partial q}{\partial u} |_{(u^*, v^*)}$, $q_v = \frac{\partial q}{\partial v} |_{(u^*, v^*)}$, with $\frac{1}{1 - \nu^* \eta \tau q_v} |_{(u^*, v^*)} = \frac{1}{1 - \eta \tau} \triangleq \chi$. Since τ is small, we only consider $\tau < \frac{1}{d}$ (i.e. $\chi > 0$) in this paper.

Model (32) becomes:

$$\begin{cases} \frac{\partial(\delta u)}{\partial t} = f_u(\delta u) + f_v(\delta v) + D_1 \nabla^2(\delta u), \\ \frac{\partial(\delta v)}{\partial t} = \chi \left(g_u - \frac{\eta \tau f_u}{\gamma} \right) (\delta u) + \chi \left(g_v - \frac{\eta \tau f_v}{\gamma} \right) (\delta v) - \frac{\chi \eta \tau}{\gamma} D_1 \nabla^2(\delta u) + \chi D_2 \nabla^2(\delta v). \end{cases} \quad (33)$$

Assume that spatiotemporal perturbations $\delta u(x, y, t)$ and $\delta v(x, y, t)$ take the following form:

$$\delta u(x, y, t) = \delta u^* e^{\lambda t} \cos k_x x \cos k_y y, \quad \delta v(x, y, t) = \delta v^* e^{\lambda t} \cos k_x x \cos k_y y, \quad (34)$$

where λ is the growth rate of the perturbation in time t , δu^* and δv^* stand for the amplitudes, and k_x and k_y are the wavenumbers of the solutions. Inserting Eqs (34) into (33), we obtain the characteristic equation at $E^* = (u^*, v^*)$ of model (5):

$$\det(\lambda E - J_{\tau k}) = \lambda^2 - \text{tr}(J_{\tau k})\lambda + \det(J_{\tau k}) = 0, \quad (35)$$

where

$$J_{\tau k} = \begin{pmatrix} f_u - D_1 k^2 & f_v \\ \chi \left(g_u - \frac{\eta f_u}{\gamma} \right) + \frac{\eta \chi D_1 k^2}{\gamma} & \chi \left(g_v - \frac{\eta f_v}{\gamma} \right) - \chi D_2 k^2 \end{pmatrix}, \tag{36}$$

$$\text{tr}(J_{\tau k}) = f_u + \chi \left(g_v - \frac{\eta f_v}{\gamma} \right) - (\chi D_2 + D_1) k^2, \tag{37}$$

$$\det(J_{\tau k}) = \chi D_1 D_2 k^4 - \chi (D_1 g_v + D_2 f_u) k^2 + \chi (f_u g_v - f_v g_u). \tag{38}$$

Now we are interested in investigating the effects of time delay and diffusion on the dynamical [system \(5\)](#), and we want to know under what conditions for time delay to destabilize the steady state and let the spatiotemporal instability occur. The onset of Turing instability requires at least one of $\text{tr}(J_{\tau k}) < 0$ and $\det(J_{\tau k}) > 0$ is violated. So we consider the emergence of the Turing instability in the following two cases:

1. $\det(J_{\tau k}) > 0$ is violated.
2. $\text{tr}(J_{\tau k}) < 0$ is violated.

Diffusion induced instability

In this part, we will consider the first case, i.e. $\det(J_k) > 0$ is violated, namely, $\det(J_{\tau k}) < 0$. It can be seen from [Eq \(38\)](#) that $\det(J_{\tau k}) = \chi \det(J_k)$ and $\chi > 0 \left(\tau < \frac{1}{\eta} \right)$, so the sign of $\det(J_{\tau k})$ is the same as $\det(J_k)$. From [Eq \(23\)](#), $\det(J_k) < 0$ is equivalent to:

$$D_2 f_u + D_1 g_v > 0, \tag{39}$$

$$(D_2 f_u + D_1 g_v)^2 > 4 D_1 D_2 (f_u g_v - f_v g_u), \tag{40}$$

at the critical value of wavenumber $k_c^2 = \frac{D_1 f_u + D_2 g_v}{2 D_1 D_2} > 0$.

In addition, $\text{tr}(J_{\tau k}) < 0$ equals to $f_u + \chi \left(g_v - \frac{\eta f_v}{\gamma} \right) < 0$. Because that $-\frac{\eta f_v}{\gamma} - f_u \eta = \det(J) > 0$, simple algebraic computation leads to:

$$0 \leq \tau < -\frac{f_u + g_v}{-\frac{\eta f_v}{\gamma} - f_u \eta} \triangleq \tau_c. \tag{41}$$

Hence, in this case, τ must satisfy

$$\tau < \min \left(\tau_c, \frac{1}{\eta} \right). \tag{42}$$

Finally, we can get the condition of diffusion induced instability:

1. When [system \(3\)](#) has three equilibria, if condition Eqs [\(11\)](#), [\(13\)](#), [\(14\)](#), [\(19\)](#), [\(39\)](#), [\(40\)](#), and [\(42\)](#) hold, then instability of [model \(5\)](#) induced by diffusion occurs.
2. When [system \(3\)](#) has two equilibria, if condition Eqs [\(11\)](#), [\(15\)](#), [\(16\)](#), [\(19\)](#), [\(39\)](#), [\(40\)](#) and [\(42\)](#) hold, then instability of [model \(5\)](#) induced by diffusion occurs.
3. When [system \(3\)](#) has a unique equilibrium, if condition Eqs [\(11\)](#), [\(18\)](#) (or [\(13\)](#) and [\(17\)](#)), [\(19\)](#), [\(39\)](#), [\(40\)](#) and [\(42\)](#) hold, then instability of [model \(5\)](#) induced by diffusion occurs.

Delay induced instability

In this part, we will consider the seconde case, i.e. $\text{tr}(J_{\tau k}) < 0$ is violated. In order to find suitable values of parameters for our simulation, we assume $\chi < 0$ ($\tau > \frac{1}{\eta}$) in this part. Following the same analysis in subsection B, $\text{tr}(J_{\tau k}) < 0$ is violated when $f_u + \chi \left(g_v - \frac{\eta f_v}{\gamma} \right) > 0$, which yields

$$\tau < -\frac{f_u + g_v}{-\frac{\eta f_v}{\gamma} - f_u \eta} \triangleq \tau_c. \tag{43}$$

Hence, in this case, τ must satisfy:

$$\frac{1}{\eta} < \tau < \tau_c. \tag{44}$$

We mainly consider the delay induced instability, therefore we keep $\det(J_{\tau k}) > 0$, which is equivalent to the same condition as Eqs (39) and (40).

At last, we can get the condition of delay induced instability:

1. When system (3) has three equilibria, if condition Eqs (11), (13), (14), (19), (39), (40) and (44) hold, then instability of model (5) induced by delay occurs.
2. When system (3) has two equilibria, if condition Eqs (11), (15), (16), (19), (39), (40) and (44) hold, then instability of model (5) induced by delay occurs.
3. When system (3) has a unique equilibrium, if condition Eqs (11), (18) (or (13) and (17)), (19), (39), (40) and (44) hold, then instability of model (5) induced by delay occurs.

In this section, we will perform numerical simulations for model (5) on the 100×100 square lattices with Neumann boundary conditions. The simulations are initiated with small amplitude random perturbations around the positive equilibrium point $E(u^*, v^*)$. The reaction-diffusion equations in our models are analyzed numerically employing Forward Difference implicit difference scheme. We set the time step $\Delta t = 0.005$, spatial mesh size $h = 1$.

We run the simulations until they reach a stationary state which indicates that the behavior does not seem to change its characteristic anymore. As a result, we only make analysis of pattern formation to one distribution(in this paper, we show the distribution of the predator).

Numerical results

A. Pattern formation induced by diffusion. In this subsection, we will focus on the pattern formation induced by diffusion, we obtain nine different types of patterns in Fig 4, where prey and predator can coexist.

In Fig 4(a) we take the parameters as

$$\begin{aligned} \eta = 0.6, \quad \tau = 0.4, \quad D_1 = 0.2, \quad D_2 = 8, \\ u^* = 0.14, \quad v^* = 22.39685714, \quad \epsilon = 135, \quad \gamma = 0.006250877036. \end{aligned} \tag{45}$$

Fig 4(a) is the typical spot pattern, which shows that the distribution of the predator v is the isolated regions with high density.

In Fig 4(b) we take the parameters as

$$\begin{aligned} \eta = 0.6, \quad \tau = 0.4, \quad D_1 = 0.2, \quad D_2 = 8, \\ u^* = 0.35, \quad v^* = 24.60714285, \quad \epsilon = 100, \quad \gamma = 0.01422351234. \end{aligned} \tag{46}$$

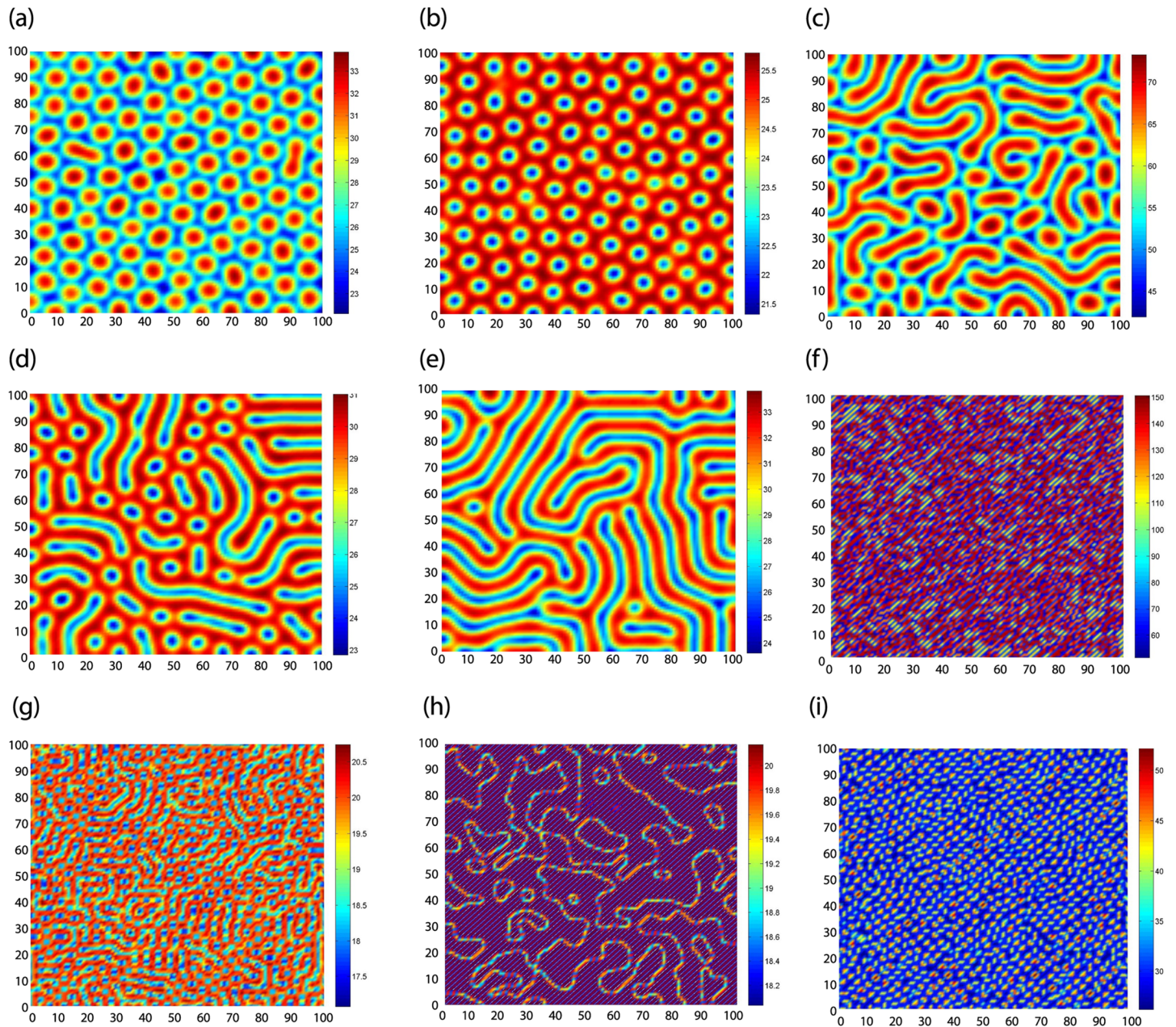


Fig 4. Nine types of patterns induced by diffusion.

doi:10.1371/journal.pone.0150503.g004

[Fig 4\(b\)](#) is the typical hole pattern, which shows that the distribution of the predator v is the isolated regions with low density.

In [Fig 4\(c\)](#) we take the parameters as

$$\begin{aligned} \eta &= 0.6, \quad \tau = 0.4, \quad D_1 = 0.2, \quad D_2 = 8, \\ u^* &= 0.11, \quad v^* = 36.48190910, \quad \epsilon = 290, \quad \gamma = 0.003015193084. \end{aligned} \tag{47}$$

[Fig 4\(c\)](#) is the mixture of red stripes and red spots named as mixed pattern 1.

In Fig 4(d) we take the parameters as

$$\begin{aligned} \eta &= 0.6, \quad \tau = 0.4, \quad D_1 = 0.2, \quad D_2 = 8, \\ u^* &= 0.3, \quad v^* = 27.53333333, \quad \epsilon = 120, \quad \gamma = 0.01089588378. \end{aligned} \tag{48}$$

Fig 4(d) is the mixture of blue stripes and blue spots named as mixed pattern 2.

In Fig 4(e) we take the parameters as

$$\begin{aligned} \eta &= 0.6, \quad \tau = 0.4, \quad D_1 = 0.2, \quad D_2 = 8, \\ u^* &= 0.25, \quad v^* = 27.37500000, \quad \epsilon = 130, \quad \gamma = 0.009132420091. \end{aligned} \tag{49}$$

Fig 4(e) is the stripe pattern.

In Fig 4(f) we take the parameters as

$$\begin{aligned} \eta &= 0.6, \quad \tau = 0.4, \quad D_1 = 0.01, \quad D_2 = 0.3, \\ u^* &= 0.2, \quad v^* = 100.00000000, \quad \epsilon = 600, \quad \gamma = 0.00200000. \end{aligned} \tag{50}$$

Fig 4(f) is somewhat like labyrinth pattern.

In Fig 4(g) we take the parameters as

$$\begin{aligned} \eta &= 0.6, \quad \tau = 0.4, \quad D_1 = 0.04, \quad D_2 = 0.16, \\ u^* &= 0.3, \quad v^* = 19.13333333, \quad \epsilon = 80, \quad \gamma = 0.01567944251. \end{aligned} \tag{51}$$

Fig 4(g) is somewhat like grid pattern.

In Fig 4(h) we take the parameters as

$$\begin{aligned} \eta &= 0.6, \quad \tau = 0.4, \quad D_1 = 0.01, \quad D_2 = 0.33, \\ u^* &= 0.3, \quad v^* = 19.13333333, \quad \epsilon = 80, \quad \gamma = 0.01567944251. \end{aligned} \tag{52}$$

Fig 4(h) is the composed parallel lines.

In Fig 4(i) we take the parameters as

$$\begin{aligned} \eta &= 0.6, \quad \tau = 0.4, \quad D_1 = 0.02, \quad D_2 = 0.54, \\ u^* &= 0.11, \quad v^* = 27.67090909, \quad \epsilon = 200, \quad \gamma = 0.003975294040. \end{aligned} \tag{53}$$

Fig 4(i) is somewhat butterfly-like patten.

B. Pattern formation induced by delay. In this subsection, we will focus on the pattern formation induced by delay, we obtain three different types of patterns in Fig 5.

In Fig 5(a) we take the parameters as

$$\begin{aligned} \eta &= 1, \quad \tau = 1.2, \quad D_1 = 0.002, \quad D_2 = 0.1, \\ u^* &= 0.3, \quad v^* = 19.13333333, \quad \epsilon = 80, \quad \gamma = 0.01567944251. \end{aligned} \tag{54}$$

Fig 5(a) is spirals 1.

In Fig 5(b) we take the parameters as

$$\begin{aligned} \eta &= 0.8, \quad \tau = 1.5, \quad D_1 = 0.002, \quad D_2 = 0.08, \\ u^* &= 0.3, \quad v^* = 52.73333334, \quad \epsilon = 240, \quad \gamma = 0.005689001264. \end{aligned} \tag{55}$$

Fig 5(b) is spirals 2.

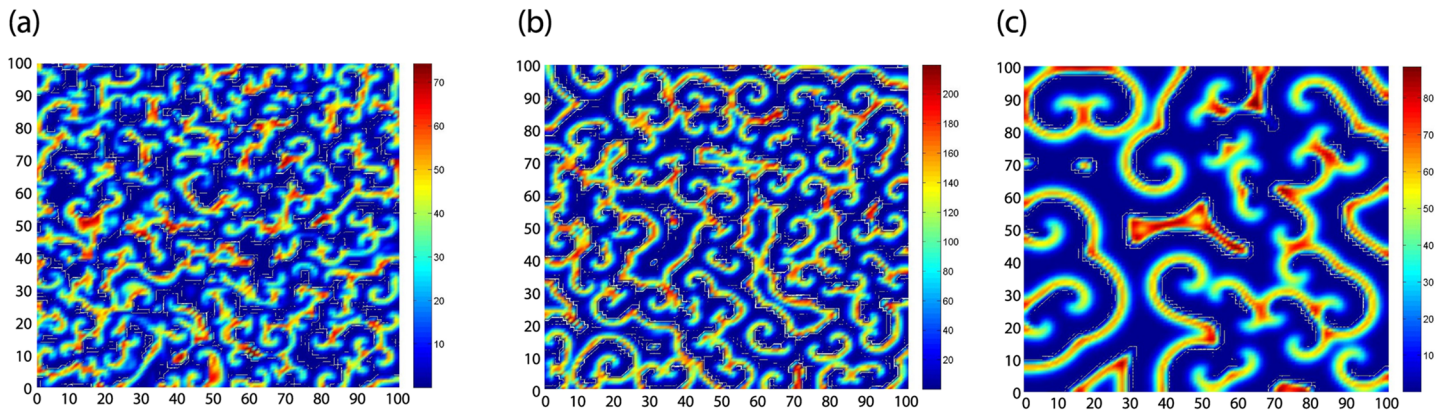


Fig 5. Three types of spirals induced by delay.

doi:10.1371/journal.pone.0150503.g005

In [Fig 5\(c\)](#) we take the parameters as

$$\begin{aligned} \eta = 0.85, \quad \tau = 1.5, \quad D_1 = 0.01, \quad D_2 = 0.38, \\ u^* = 0.3, \quad v^* = 19.13333333, \quad \epsilon = 80, \quad \gamma = 0.01567944251. \end{aligned} \tag{56}$$

[Fig 5\(c\)](#) is spirals 3.

Discussion

In this paper, a spatial Leslie type predator-prey system with Holling type III functional response and time delay has been investigated. To well understand the impact of delay and diffusion on the instability, we have made theoretical analysis and numerical simulations. Since the equilibrium cannot be expressed in a useful closed form, we cannot discuss its qualitative properties in normal routine. Firstly, we discuss the number and qualitative properties of positive equilibrium via the original parameters. Secondly, we obtain conditions of two types of instability: diffusion induced instability and delay induced instability. Finally, numerical simulations are performed to illustrate the theoretical findings. Both the theoretical and numerical results reveal that the interaction between time delay and diffusion can give rise to stationary patterns.

However, it should be noted that the method in this paper is only suitable for short time delay τ . When the delay is large, one should use other methods to find the condition for Turing instability. Moreover, we may investigate travelling wave of [model \(5\)](#) in the future study. It should be also worth pointing that other types of instability may be found in [system \(5\)](#). For example, we can use normal formal theory and the center manifold theorem of partial functional differential equations to analyze the Hopf bifurcation of [system \(5\)](#) [3].

Supporting Information

S1 File. Qualitative properties and stability of the interior equilibria of [system \(3\)](#).
(PDF)

Author Contributions

Conceived and designed the experiments: CW LC. Performed the experiments: HL. Analyzed the data: CW HL. Contributed reagents/materials/analysis tools: CW LC HL. Wrote the paper: CW LC HL.

References

1. Wollkind DJ, Collings JB, Logan JA. Metastability in a temperature-dependent model system for predator-prey mite outbreak interactions on fruit trees. *Bull. Math. Biol.* 1988; 50(4):379–409.
2. Hsu SB, Huang TW. Global Stability For A Class Of Predator-Prey Systems. *Siam J. Appl. Math.* 1995; 55(3):763–783. doi: [10.1137/S0036139993253201](https://doi.org/10.1137/S0036139993253201)
3. Sun GQ, Wang SL, Ren Q, Jin Z, Wu YP. Effects of time delay and space on herbivore dynamics: linking inducible defenses of plants to herbivore outbreak. *Scientific Reports* 2015; 5:11246. doi: [10.1038/srep11246](https://doi.org/10.1038/srep11246) PMID: [26084812](https://pubmed.ncbi.nlm.nih.gov/26084812/)
4. Jones LE, Ellner SP. Evolutionary tradeoff and equilibrium in an aquatic predator-prey system. *Bull. Math. Biol.* 2004; 66(6):1547–1573. doi: [10.1016/j.bulm.2004.02.006](https://doi.org/10.1016/j.bulm.2004.02.006) PMID: [15522345](https://pubmed.ncbi.nlm.nih.gov/15522345/)
5. Guan XN, Wang WM, Cai YL. Spatiotemporal dynamics of a Leslie-Gower predator-prey model incorporating a prey refuge. *Nonlinear Analysis Real World Applications* 2011; 12(4):2385–2395. doi: [10.1016/j.nonrwa.2011.02.011](https://doi.org/10.1016/j.nonrwa.2011.02.011)
6. Sun GQ, Wu ZY, Wang Z, Jin Z. Influence of isolation degree of spatial patterns on persistence of populations. *Nonlinear Dynam.* 2016; 83:811–819. doi: [10.1007/s11071-015-2369-6](https://doi.org/10.1007/s11071-015-2369-6)
7. Jost C. Comparing predator-prey models qualitatively and quantitatively with ecological time-series data. Ph.D. thesis. Paris Grignon: Institute National Agronomique; 1998.
8. Bazykin AD. *Nonlinear Dynamics of Interacting Populations*. Singapore: World Scientific Publishing, 1998.
9. Leslie PH. Some further notes on the use of matrices in population mathematics. *Biometrika* 1948; 35:213–245. doi: [10.1093/biomet/35.3-4.213](https://doi.org/10.1093/biomet/35.3-4.213)
10. Leslie PH, Cower JC. The properties of a stochastic model for the predator-prey type of interaction between two species. *Biometrika* 1960; 47:219–234. doi: [10.1093/biomet/47.3-4.219](https://doi.org/10.1093/biomet/47.3-4.219)
11. Freedman HI, Mathsen RM. Persistence in predator-prey systems with ratio-dependent predator influence. *Bull. Math. Biol.* 1993; 55:817–827. doi: [10.1007/BF02460674](https://doi.org/10.1007/BF02460674)
12. Hsu SB, Huang TW. Global stability for a class of predator-prey system. *SIAM J. Appl. Math.* 1995; 55:763–783. doi: [10.1137/S0036139993253201](https://doi.org/10.1137/S0036139993253201)
13. Segel L and Jackson J. Dissipative structure: an explanation and an ecological example. *J. Theor. Biol.* 1972; 37:545–559. doi: [10.1016/0022-5193\(72\)90090-2](https://doi.org/10.1016/0022-5193(72)90090-2) PMID: [4645361](https://pubmed.ncbi.nlm.nih.gov/4645361/)
14. Sun GQ, Jin Z, Li L and Li BL. Self-organized wave pattern in a predator-prey model. *Nonlinear Dynam.* 2010; 60:265–275. doi: [10.1007/s11071-009-9594-9](https://doi.org/10.1007/s11071-009-9594-9)
15. Levin S, Segel L. Hypothesis for origin of planktonic patchiness. *Nature* 1976; 259(5545):659–659. doi: [10.1038/259659a0](https://doi.org/10.1038/259659a0)
16. Sun GQ, Jin Z, Liu QX, Li L. Dynamical complexity of a spatial predator-prey model with migration. *Ecol. Model.* 2008; 219:248–255. doi: [10.1016/j.ecolmodel.2008.08.009](https://doi.org/10.1016/j.ecolmodel.2008.08.009)
17. Sengupta A, Kruppa T, Lowen H. Chemotactic predator-prey dynamics. *Phys. Rev. E* 2011; 83(3):1133–1144. doi: [10.1103/PhysRevE.83.031914](https://doi.org/10.1103/PhysRevE.83.031914)
18. Sun GQ, Zhang J, Song LP, Jin Z, Li BL. Pattern formation of a spatial predator-prey system. *Appl. Math. Comput.* 2012; 218:11151–11162. doi: [10.1016/j.amc.2012.04.071](https://doi.org/10.1016/j.amc.2012.04.071)
19. Cushing JM. *Integrodifferential equations and delay models in population dynamics*. Heidelberg: Springer-Verlag, 1997.
20. Kuang Y. *Delay differential equations with application in population dynamics*. New York: Academic Press, 1993.
21. Nindjin AF, Aziz-Alaoui MA, Cadivel M. Analysis of a predator-prey model with modified Leslie-Gower and Holling-type II schemes with time delay. *Nonlinear Anal. Real World Appl.* 2006; 7:1104–1108. doi: [10.1016/j.nonrwa.2005.10.003](https://doi.org/10.1016/j.nonrwa.2005.10.003)
22. Xu R and Chen LS. Persistence and stability for a two-species ratio-dependent predator-prey system with time delay in a two-patch environment. *Comput. Math. Appl.* 2000; 40(0):577–588.
23. Yafia R, Adnani F, Alaoui H. Limit cycle and numerical simulations for small and large delays in a predator-prey model with modified Leslie-Gower and Holling-type II schemes. *Nonlinear Anal.: Real World Appl.* 2008; 9(5):2055–206. doi: [10.1016/j.nonrwa.2006.12.017](https://doi.org/10.1016/j.nonrwa.2006.12.017)
24. Ruan S. On nonlinear dynamics of predator-prey models with discrete delay. *Math. Modelling Nature Phenom.* 2009; 4(2):140–188. doi: [10.1051/mmnp/20094207](https://doi.org/10.1051/mmnp/20094207)
25. Faria T. Stability and bifurcation for a delayed predator-prey model and the effect of diffusion. *Math. Anal. Appl.* 2001; 254:433–463. doi: [10.1006/jmaa.2000.7182](https://doi.org/10.1006/jmaa.2000.7182)

26. Haderer KP, Ruan S. Interaction of diffusion and delay. *Discrete Contin. Dyn. Syst. B* 2007; 8:95–105. doi: [10.3934/dcdsb.2007.8.95](https://doi.org/10.3934/dcdsb.2007.8.95)
27. Yang XP. Stability and Hopf bifurcation for a delayed prey-predator system with diffusion effects. *Appl. Math. Comput.* 2007; 192:552–566. doi: [10.1016/j.amc.2007.03.033](https://doi.org/10.1016/j.amc.2007.03.033)
28. Yan S, Lian XZ, Wang WM. Spatiotemporal dynamics in a delayed diffusive predator model. *Appl. Math. Comput.* 2013; 224:524–534. doi: [10.1016/j.amc.2013.08.045](https://doi.org/10.1016/j.amc.2013.08.045)
29. Sun GQ, Chakrabort A, Liu QX, Jin Z, Anderson KE, Li BL. Influence of time delay and nonlinear diffusion on herbivore outbreak. *Commun. Nonlinear Sci. Numer. Simulat.* 2014; 19:1507–1518. doi: [10.1016/j.cnsns.2013.09.016](https://doi.org/10.1016/j.cnsns.2013.09.016)
30. Sen S, Ghosh P, Riaz S, Ray D. Time-delay-induced instabilities in reaction-diffusion systems. *Phys. Rev. E* 2009; 80(4):2016–2023. doi: [10.1103/PhysRevE.80.046212](https://doi.org/10.1103/PhysRevE.80.046212)
31. Ghosh P. Control of the Hopf-Turing transition by time-delayed global feedback in a reaction-diffusion system. *Phys. Rev. E* 2011; 84(1):1183–1206. doi: [10.1103/PhysRevE.84.016222](https://doi.org/10.1103/PhysRevE.84.016222)
32. Hu HX, Li QS and Li. Traveling and standing patterns induced by delay feedback in uniform oscillatory reaction-diffusion system. *Chem. Phys. Lett.* 2007; 447(4):364–367. doi: [10.1016/j.cplett.2007.09.031](https://doi.org/10.1016/j.cplett.2007.09.031)
33. Li QS and Hu HX. Pattern transitions induced by delay feedback. *J. Chem. Phys* 2007; 127(15). doi: [10.1063/1.2792877](https://doi.org/10.1063/1.2792877)
34. Tang YL, Huang DQ, Zhang WN. Direct parametric analysis of an enzyme-catalyzed reaction model. *IMA Journal of Applied Mathematics* 2011; 76(6):876–898. doi: [10.1093/imamat/hxr005](https://doi.org/10.1093/imamat/hxr005)
35. Sun GQ, Jin Z, Liu QX, Li L. Pattern formation in a spatial S-I model with non-linear incidence rates. *J. Stat. Mech.* 2007; 11:1101.
36. Sun GQ, Jin Z, Liu QX, Li L. Chaos induced by breakup of waves in a spatial epidemic model with non-linear incidence rate. *J. Stat. Mech.* 2008; 8:08011. doi: [10.1088/1742-5468/2008/08/P08011](https://doi.org/10.1088/1742-5468/2008/08/P08011)
37. Aragón JL, Torres M, Gil D, Barrio RA, Maini PK. Turing patterns with pentagonal symmetry. *Phys. Rev. E* 2002; 65(10):051913.
38. Sun GQ, Jin Z, Li L, Haque M, Li BL. Spatial patterns of a predator-prey model with cross diffusion. *Nonlinear Dyn.* 2012; 69:1631–1638.
39. Murray DJ. *Mathematical Biology II: Spatial Models and Biomedical Applications*. Berlin: Springer; 2003.